Geophysical Journal International

The quest for a consistent signal in ground and GRACE gravity time-series

Michel Van Camp,[1] Olivier de Viron,[2] Laurent Métivier,[3] Bruno Meurers[4] and Olivier Francis[5]

[1]*Royal Observatory of Belgium, 3 avenue Circulaire, B-1180 Brussels, Belgium. E-mail: m.vancamp@oma.be*
[2]*Institut de Physique du Globe de Paris (IPGP, Sorbonne Paris-Cité, UMR 7154, CNRS, Université Paris-Diderot), bâtiment Lamarck, Case 7011, 35 rue Hélène Brion, F-75013 Paris, France*
[3]*Institut National de l'Information Géographique et Forestière/Laboratoire de Recherche en Géodésie, Université Paris-Diderot, bâtiment Lamarck, case 7011, 35 rue Hélène Brion, F-75013 Paris, France*
[4]*Department of Meteorology & Geophysics, University of Vienna, Althanstrasse 14, UZA II, 2D504, A-1090 Vienna, Austria*
[5]*Faculté des Sciences, de la Technologie et de la Communication, University of Luxembourg, 6, rue Richard Coudenhove-Kalergi, L-1359 Luxembourg*

SUMMARY
Recent studies show that terrestrial and space-based observations of gravity agree over Europe. In this paper, we compare time-series of terrestrial gravity (including the contribution due to surface displacement) as measured by superconducting gravimeters (SGs), space-based observations from Gravity Recovery and Climate Experiment (GRACE) and predicted changes in gravity derived from two global hydrological models at 10 SG stations in central Europe. Despite the fact that all observations and models observe a maximum in the same season due to water storage changes, there is little agreement between the SG time-series even when they are separated by distances smaller than the spatial resolution of GRACE. We also demonstrate that GRACE and the SG observations and the water storage models do not display significant correlation at seasonal periods nor at interannual periods. These findings are consistent with the fact that the SGs are sensitive primarily to mass changes in the few hundred metres surrounding the station.

Key words: Satellite geodesy; Time variable gravity; Hydrology; Europe.

1 INTRODUCTION

The Earth is a coupled dynamic system with a climate component composed of the atmosphere, the oceans, the cryosphere and the continental hydrology. The sensitivity of contemporary geodetic techniques to the Earth system makes them a powerful and indispensable tool to monitor its dynamics. Nevertheless, the contribution of geodesy to understanding the Earth relies on the accuracy and quality of the data analysis. In particular, geodetic theory has to be improved to the extent that we can take full advantage of the data precision. For example, estimate the hydrological effects on terrestrial and space gravity measurements remains challenging, as subsurface water dynamics is very difficult to assess, at both local and global scales.

Separation of the couplings can be achieved by benefiting from the combination of multiple geodetic measurements and/or of the climate models. Various studies showed a fair consistency between Global Navigation Satellite Systems (GNSS), climate models and Gravity Recovery and Climate Experiment (GRACE) data (Blewitt *et al.* 2001; Blewitt & Clarke 2003; van Dam *et al.* 2007; Tregoning & Watson 2009; Tesmer *et al.* 2011; Valty *et al.* 2013). Here, we evaluate the insights that can be obtained from a comparison/combination of terrestrial gravity measurements from super-

conducting gravimeters (SGs) in central Europe with the equivalent gravity estimated from the GRACE solutions. Previous studies (e.g. Neumeyer *et al.* 2006, 2008; Weise *et al.* 2009, 2011; Abe *et al.* 2012; Crossley *et al.* 2012) claim that a common behaviour was found between the times-series from the SGs, GRACE and hydrological models.

However, regarding the Newtonian effect of hydrological processes, SGs are sensitive primarily to mass included in the few hundred metres around the station (Creutzfeldt *et al.* 2008). So, one may have expected larger discrepancies between the SGs and GRACE solutions. To address this problem, we extend the previous study both in time—time-series of our study extend up to 2012—and in the number of SG used, and we test, using a different method, the robustness of the common signal.

2 DATA

2.1 Superconducting gravimeters

The SG station locations are shown in the map of Fig. 1, and their characteristics are described in Table 1. The time-series are corrected for tidal effects using the parameter sets obtained from the tidal analysis of the hourly time-series. This analysis was performed
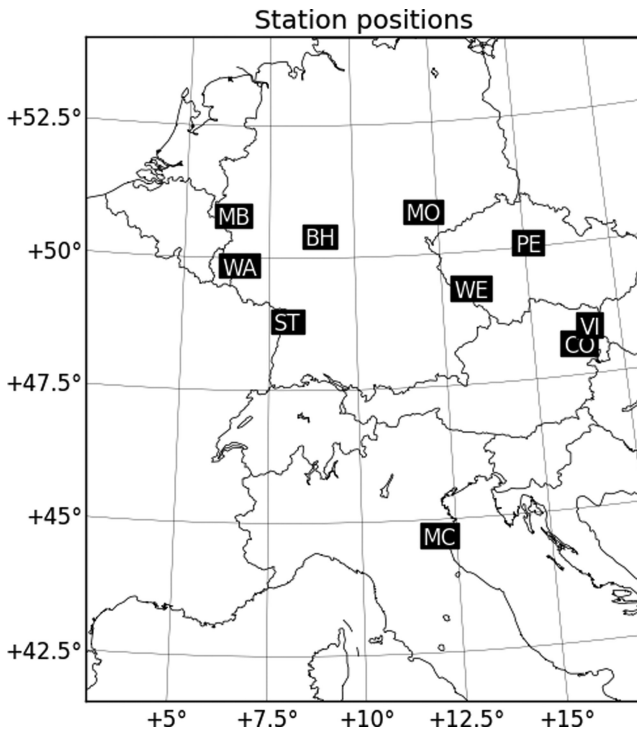
Station positions

Figure 1. Map showing the location of the SG stations used in this study, see Table 1 for details.

with the Eterna 3.4 package (Wenzel 1996). The atmospheric influence is removed using the 3-D high-resolution 3-hrly European Centre for Medium-Range Weather Forecasts (ECMWF) model, assuming an inverted barometer hypothesis, as provided by J.-P. Boy (http://loading.u-strasbg.fr/GGP/)—for a review of the 3-D correction, see Crossley *et al.* (2013). The centrifugal effect associated with polar motion is also corrected (Wahr 1985).

Removal of instrumental offsets is a critical step and is probably the most subjective part of the SG processing, as this depends on the operator (Hinderer *et al.* 2007). For all stations, the offsets are removed either visually, when the gap is not too long (typically, no more than a few hours), or, if the gap is longer, adjusting the SG series using colocated absolute gravimeter measurements when available. For the Pecny (PE), Moxa (MO) and Strasbourg (ST) stations, our processing was found consistent with the residuals provided by the operators; for the other stations the operators provided the data directly. The accumulated impact of remaining differences in the offsets is similar to a random walk process (Hinderer *et al.* 2007), and is included in the instrumental drift. For

all series, after corrections, a second-order polynomial was adjusted and subtracted to remove possible non-linear instrumental drift or other very long term geophysical effects, which are out of the scope of this study.

The SG time-series used in this study are shown in Figs 2(a) and (b) after removing a composite seasonal cycle by means of a stacking technique (Hartmann & Michelsen 1989). This tool allows removing the mean signal of period *T*. This is done on each SG series separately, by first computing the mean signal for a given phase ϕ by averaging all the value of the time-series corresponding to this phase ($t = \phi$, $T + \phi$, $2T + \phi$, . . .), then by removing it at every data point of this phase. At Wettzell, a change in the annual signal is observed after 2008, probably caused by major construction works undertaken in 2009 and by the fact that the SG was moved by 250 m in 2010 October.

2.2 Global hydrological models

We use hydrological loading effects provided by J.-P. Boy (Boy & Hinderer 2006; http://loading.u-strasbg.fr/GGP/), computed from the continental ground water content provided by the GLDAS/Noah model (Rodell *et al.* 2004) and ERA interim reanalysis (Uppala *et al.* 2005). Those data sets will be referred to as GLDAS and ERA, here after. The 6-hrly model based on ERA are interpolated to 3-hrly data to match the SG and GLDAS sampling. The space sampling of GLDAS is 0.25° and 0.7° for ERA interim (Boy, Personal Communication, 2012). The hydrology grids were decomposed into spherical harmonics, and then converted into ground gravity using the appropriate combination of load Love Number (e.g. Farrell 1972). The Love numbers were calculated assuming PREM model (Dziewonski & Anderson 1981) as Earth model.

2.3 GRACE

We use GRACE time gravity solutions from seven institutes, as summarized in Table 2:

- The release 5 of the three official solutions, NASA/CSR, NASA/JPL and GFZ groups (noted here as CSR, JPL and GFZ). These solutions are given without filtering but corrected for a dealiasing model for atmosphere and oceans (AOD dealiasing products).
- Four other independent solutions: ITG monthly solution from Bonn university (Kurtenbach *et al.* 2009), AIUB monthly solution from Bern university (e.g. Beutler *et al.* 2010), DTM-1b monthly solution from Delft University of Technology (noted here DTM,

Table 1. Description of the SG time-series used in this study.

| Acronym	Name	Instrument	Latitude	Longitude	Starting time	Ending time
BH	Bad Homburg	CD030 L	50.2285	8.6113	2002 January 5	2007 April 1
		SG044			2007 April 1	2012 June 1
CO	Conrad	C025	47.9288	15.8609	2007 November 14	2012 May 28
MC	Medicina	C023	44.5219	11.6450	2002 January 5	2012 June 1
MB	Membach	C021	50.6092	6.0067	2002 January 5	2012 May 3
MO	Moxa	C034 L	50.6447	11.6156	2002 January 5	2011 December 27
PE	Pecny	OSG-050	49.9138	14.7856	2007 May 6	2011 December 15
ST	Strasbourg	C026	48.6217	7.6850	2002 January 5	2010 December 27
VI	Vienna	C025	48.2493	16.3579	2002 January 5	2007 October 23
WA	Walferdange	OSG-040	49.6647	6.1528	2003 December 23	2012 May 28
WE	Wettzell	CD-029 L	49.1440	12.8780	2002 January 5	2010 October 10
		SG-030			2010 October 10	2012 June 30
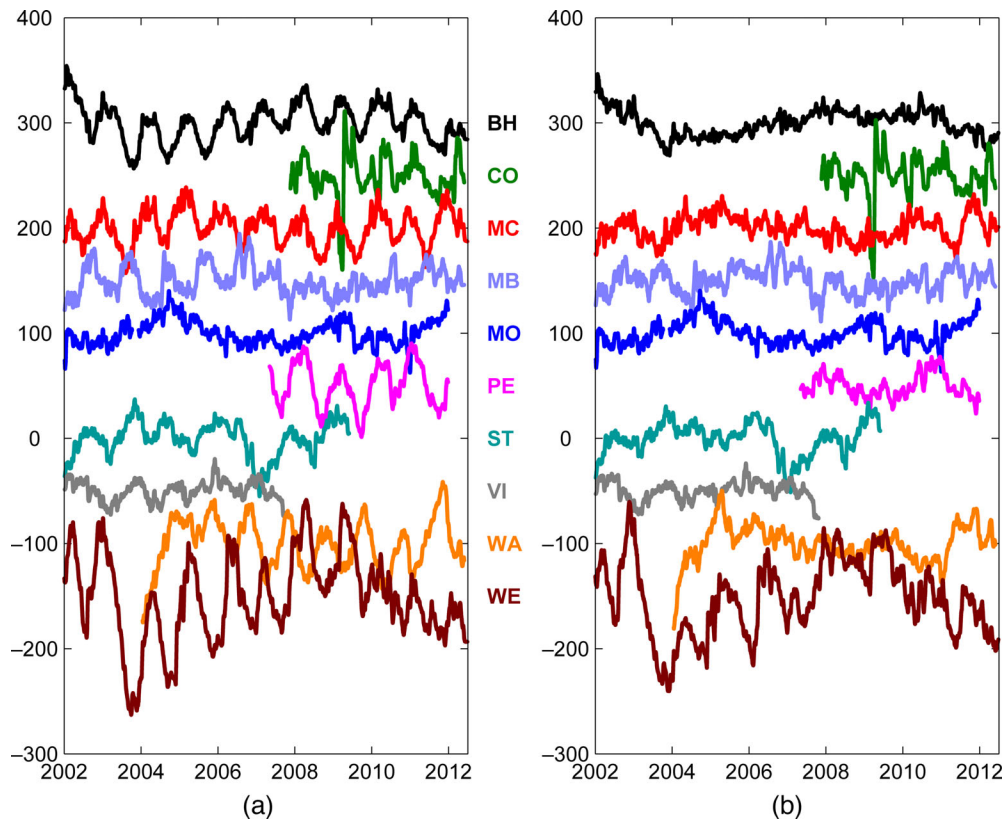
Figure 2. SG time-series after correcting for tidal, atmospheric, polar motion and instrumental drift effects before (a) and (b) after removing a composite annual cycle. The stations series are sorted alphabetically from top to bottom.

Table 2. Summary of the different GRACE solutions used in this study.

Solution name	Origin	Reference geoid	Time period	Periodicity	Additional filtering	Non-tidal ocean load added	Note
CSR	NASA Center for Space Research (USA)	GGM03C	2004–2010	Monthly	Destriping	No	Data access from http://podaac.jpl.nasa.gov/
JPL	NASA Jet Propulsion Laboratory (USA)	GGM03C	2004–2010	Monthly	Destriping	No	Data access from http://podaac.jpl.nasa.gov/
GFZ	GFZ German Research Centre for Geosciences (Germany)	EIGEN-6S	2005–2010	Monthly	Destriping	No	Dahle *et al*. (2012)
ITG	Bonn University (Germany)	ITG-GRACE2010S	2002–2009	Monthly	Destriping	No	Kurtenbach *et al*. (2009)
AIUB	Bern University (Germany)	AIUB-GRACE03S	2003–2009	Monthly	Destriping	No	Degree 2 zonal coefficient corrected. Beutler *et al*. (2010)
GRGS	CNES French Spatial Agency - GRGS group (France)	EIGEN-GRGS.RL02.MEAN-FIELD	2002–2012	10-d	None	No	Regularized solution. Bruinsma *et al*. (2009)
DTM	Delft University of Technology (Netherlands).	EIGEN-GL04C	2003–2010	Monthly	None	No	DTM-1b model. Liu *et al*. (2010). Wiener filter based solution (Klees *et al*. 2008).
GFZ_O	See GFZ	See GFZ		See GFZ	See GFZ	Yes	See GFZ
GRGS_O	See GRGS	See GRGS		See GRGS	See GRGS	Yes	See GRGS
ITG_O	See ITG	See ITG		See ITG	See ITG	Yes	See ITG

Liu *et al*. 2010) and GRGS 10-d release 2 solution from the CNES French space agency (Bruinsma *et al*. 2009).

The GRGS and DTM solutions are already regularized using various methods (see above references and websites for more details). In the CSR, JPL, GFZ, ITG and AIUB series, striping noise has to

be filtered out prior to investigations. We applied a correlated-error filter and a 500-km Gaussian smoothing based on the Swenson & Wahr (2006) method; this method was shown as the most precise in Valty *et al*. (2013). We found that AIUB solution presents an anomalously high degree 2 zonal coefficient. Since this coefficient is usually very small in surface gravity time variations (unlike the

geoid that presents large J2 time variations), it has been suppressed from the AIUB solution prior to our computation.

To allow comparison between GRACE solutions and ground gravity measurements, which here are not corrected for the non-tidal ocean contribution, we also make a comparison with the three GRACE solutions where the non-tidal ocean contribution has been added back using dealiasing products, when provided by the analysis centre (only GRGS, GFZ and ITG). A total of 10 GRACE solutions has consequently been used. As for the hydrology models, GRACE time-variable gravity was decomposed into spherical harmonics, and then reconstructed at the SG station location as ground gravity values, using the appropriate combination of load Love numbers. Note that we did not use the classical formulation for gravity perturbation based on the loading gravimetric factor (see Farrell 1972 or Boy *et al.* 2002), because it supposes that the load is above the gravimeter. Such assumption is valid for the atmosphere or oceans, but is less adapted for hydrology loading problems, where the load is generally under the sensor. We prefer the formulation used by Crossley *et al.* (2012), which is the derivative of the gravitational potential perturbation inferred from GRACE measurements plus a free air additional correction due to ground displacements. If we note $(\Delta C_{nm}, \Delta S_{nm})$ the Stoke's coefficients of degree n and order m of the gravitational potential perturbation provided by GRACE, h_n the vertical displacement Love number and k_n the potential perturbation Love number, then the gravimetric signal can be reconstructed as follows:

$$g(\theta, \lambda, t) = \frac{GM}{a^2} \sum_{n=2}^{N} \sum_{m=0}^{+n} P_n^m(\cos\theta) \left(n + 1 - 2\frac{h_n}{1+k_n} \right)$$
$$\times \left[\Delta C_{nm}(t)\cos(m\lambda) + \Delta S_{nm}(t)\sin(m\lambda) \right],$$

where P_n^m are the associated Legendre polynomials, GM is Earth's standard gravitational parameter, a the semi-major axis of the ellipsoid, N the maximum degree and (θ, λ, t) are colatitude, longitude and time.

The 3-hrly time-series of SG and hydrological models are decimated to 5 d; for GRACE, the original sampling rates were kept as provided by the different data centres, except in the case of the Empirical Orthogonal Function (EOF) analysis, where the GRACE series were linearly interpolated to 5 d to compare directly with the SG data. Scaling the series to the shortest sample interval avoids losing information. Before performing the different analyses, a second-degree polynomial was systematically adjusted to all the SG, hydrological and GRACE series, in order to remove any possible bias that may be caused by non-linear slopes caused by SG instrumental drift or by residual long-period geophysical signals which are beyond the scope of this paper (Van Camp & Francis 2006; Van Camp *et al.* 2010).

3 COMMON VARIABILITY IN THE SG TIME-SERIES

As GRACE only sees large-scale phenomenon, any GRACE/SG agreement would rely on common variability between the SG time-series at large scale. A classical method to look for a common variability in time-series is correlation study, as done by Neumeyer *et al.* 2008 and Abe *et al.* 2012. The correlation coefficients of the series are given in Table 3. However, the interpretation of the correlation coefficient rely on a statistical test which makes no sense when a strong periodic signal is present in the data, as all the data points corresponding to the same phase are not independent (see

Table 3. Correlation (in per cent) between the different time-series shown in Fig. 2(a). Due to the strong annual component, the significance could not be tested.

	BH	CO	MB	MC	MO	PE	ST	VI	WA
CO	31	-							
MB	−53	3	-						
MC	31	1	−27	-					
MO	−35	−13	−3	17	-				
PE	93	31	−21	58	−11	-			
ST	−54	−16	9	−20	35	15	-		
VI	3	N/A	27	11	9	−49	10	-	
WA	−69	−36	37	−4	14	−70	44	−9	-
WE	78	29	−40	18	−26	55	−39	−25	−49

Von Storch & Zwiers 1999 for more detail on the assumption). As evidenced by Fig. 2(a), a strong seasonal signal is present in most of the time-series. The problem appears clearly when one takes two arbitrary signals that would be pure annual waves:

$$X_1 = \cos(2\pi vt + \varphi), \tag{1}$$

$$X_2 = \cos(2\pi vt). \tag{2}$$

If the time-series are properly sampled, the correlation coefficient is a fair approximation of $\cos(\varphi)$, meaning that even with a 45° phase difference, the correlation amounts to 0.7, which may appear as important. Actually, the correlation analysis cannot be applied when the signal is dominated by the seasonal component. The same problem will appear whatever other comparison method is used, as the presence of a strong periodic component is only significant if the detection of that period is an interesting result by itself. For example, discovering the period of the translational motion of the inner core inside the outer core (Slichter mode; Slichter 1961) in SG records would be a nice discovery. Conversely, many geodetic time-series one could take on Earth would exhibit at least some seasonal signal, and no conclusion can be drawn from such a result. One could argue that the fact that there is an annual signal in both series is significant by itself, but this is not really instructive. On the contrary, correlation studies can be insightful after removing the seasonal component from the signal. Let us look at the correlation of the time-series corrected for the annual component (Table 4 and Fig. 3); 10 pairs of 41 are significantly correlated: BH–MO, BH–PE, BH–ST, BH–WA, BH–WE, MB–VI, MB–WA, MO–PE, PE–WA and VI–WA, which is above the significance level. On the other hand, the fact that only a fourth of the pairs of time-series appear significantly correlated when the seasonal cycle is filtered out is not consistent with a dominant coherent signal at the different stations. Note that, in each significant case but one (VI–WA), underground pairs and surface pairs are correlated, while underground-surface pairs are anticorrelated. This is again consistent with the local masses playing the dominant role in SG measurements, as local water would be above the gravimeter for underground station and below it for surface station.

The EOF decomposition is a classical data mining technique, which allows retrieving common signal in a set of time-series. Technical information and algorithms can be found in Preisendorfer (1988). Starting from a set of time-series $x_i(t_l)$, $i = 1 \ldots N$, $l = 1 \ldots M$, the covariance matrix is computed, and the eigenvectors of the covariance matrix, called principal components or EOFs, are

Table 4. Correlation coefficients (significance level in per cent) as shown in Fig. 3, between the different time-series shown in Fig. 2(b). The significant correlations are bold faced. The coefficient is not evaluated when the time-series overlapping is shorter than 3.5 yr.

	BH	CO	MB	MC	MO	PE	ST	VI	WA
CO	19 (86)	-							
MB	−32 (92)	0 (51)	-						
MC	−15 (74)	0 (51)	14 (79)	-					
MO	**−52 (99)**	−27 (88)	−3 (55)	22 (87)	-				
PE	**77 (100)**	30 (91)	−14 (76)	20 (78)	**−52 (96)**	-			
ST	**−52 (98)**	N/A	−11 (71)	−3 (56)	40 (93)	N/A	-		
VI	11 (70)	N/A	**39 (96)**	1 (52)	15 (71)	N/A	13 (72)	-	
WA	**−56 (100)**	−28 (92)	**36 (96)**	20 (85)	23 (84)	**−67 (99)**	38 (93)	**−52 (100)**	-
WE	**72 (100)**	14 (80)	−26 (93)	−3 (57)	−35 (94)	17 (74)	−26 (89)	−22 (82)	−1 (52)
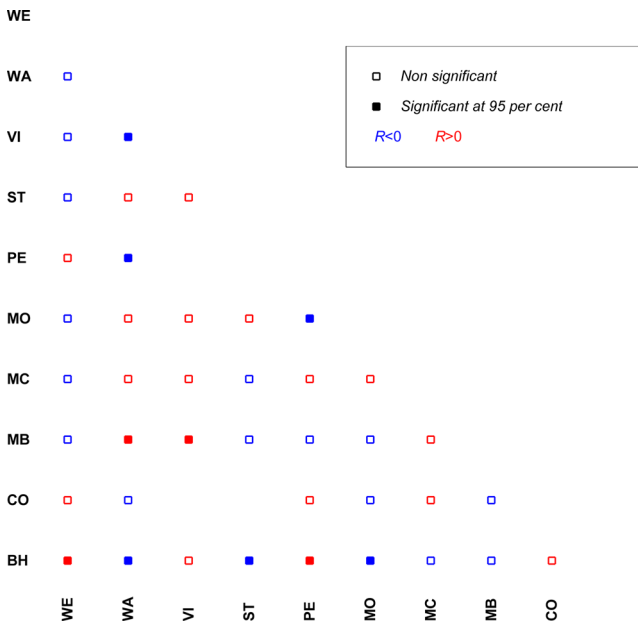
Figure 3. Correlation between the different SG time-series as in Fig. 2(b), after removing a composite annual signal. The squared are filled when the correlation is significant (95 per cent level). The coefficient is not evaluated when the time-series overlapping is shorter than 3.5 yr.

used as a new basis in which the time-series are written. Then, the time-series can be written as

$$x_i(t_l) = \sum_{k=1}^{N} \alpha_{k,i} T_k(t_l), \qquad (3)$$

where the $\alpha_{k,i}$ are the EOFs, and the functions $T_k(t_l)$ are their associated time-series. Classically, the EOFs are sorted so that the first EOF explains the most variance in the initial set of time-series. Most of the time, an important part of the variance is explained by only a few EOFs. Starting from a set of N time-series, the covariance matrix is $N \times N$; consequently, there are exactly N eigenvector for the matrix.

Let us take the seven stations as discussed in Crossley *et al.* (2012): BH, MB, MC, MO, ST, VI and WE, from 2002.6 to 2007.8; note that the annual signal was not filtered out. For the reasons explained in the beginning of this section, it is difficult to interpret the results if the series contains an annual component: the EOF analysis will extract the seasonal signal as the first mode, even with a non-negligible phase-lag (up to 45°) between the time-series. Actually, the EOF analysis then only allows concluding to the presence

of a seasonal signal in all the time-series. Here, after filtering for the seasonal cycle, we computed the eigenvectors and the associated time-series. Then, we computed the variance explained by each of the EOFs for each initial time-series. The total variance explained by the first mode over the seven SG time-series is slightly less than 30 per cent. There are three surface SGs (BH, MC and WE) where 78, 67 and 58 per cent of the variance is explained, the other four stations having less than 10 per cent explained. This result may seem encouraging, but it is important to note that the algorithm focuses on the most significant EOF mode, that is, the one that explains the most variance. To assess the significance of this result, we compare those results with what would be obtained for random time-series. Speaking of climatically induced signal, the hypothesis of a red noise described as a degree one autoregressive process (AR1) is commonly used (Ghil *et al.* 2002). We estimated the AR1 parameters for each of the SG time-series, and then generated a set of 100 000 time-series with the same parameters. We then computed the EOF decomposition of each of the 100 000 sets of seven time-series, and computed the variance explained by the first EOF mode. The results are shown in Fig. 4, which shows the distribution of the variance explained by the first mode, with a red vertical line at the value obtained with the SG data set. We observe that the variance explained by the first mode narrows the mode of the distribution obtained with random data; this indicates that the 30 per cent variance explained does not demonstrate that a common source of signal exists, it is simply due to the fact that the algorithm is built to extract the EOF in such a way that most of the variance will be explained by one time-series, whatever the input. This result is consistent with previous studies, where they show a common signal which is mostly annual, and not much beside, although that picture may change when longer series are available.

Nevertheless, the seasonal signal in the SG time-series is information that needs to be analysed. Its amplitude and phase are obtained by a linear least-square fit of a sine wave at each station. They are given in Table 5 and represented as phasor diagrams in Fig. 5(a). Given that the local water content dominates the SG gravity signal, the phasors are also provided in Fig. 5(b) with an opposite sign for the gravity data at the underground stations (CO, MB, MO, ST, VI and WA). This approach was adopted by Boy & Hinderer (2006) and Van Camp *et al.* (2010). Although the phasors are less dispersed, those diagrams show that the amplitudes and phases do not indicate a common signal, but rather station maxima within a seasonal cycle, as expected. Of course, GRACE does smooth these signals because of its much larger averaging footprint.

The magnitude of the annual signal depends on the local hydrogeological context. Even for homogeneous climate conditions, the topography around the SG stations, as well as the local petrology and the building umbrella effect, result in inhomogeneous
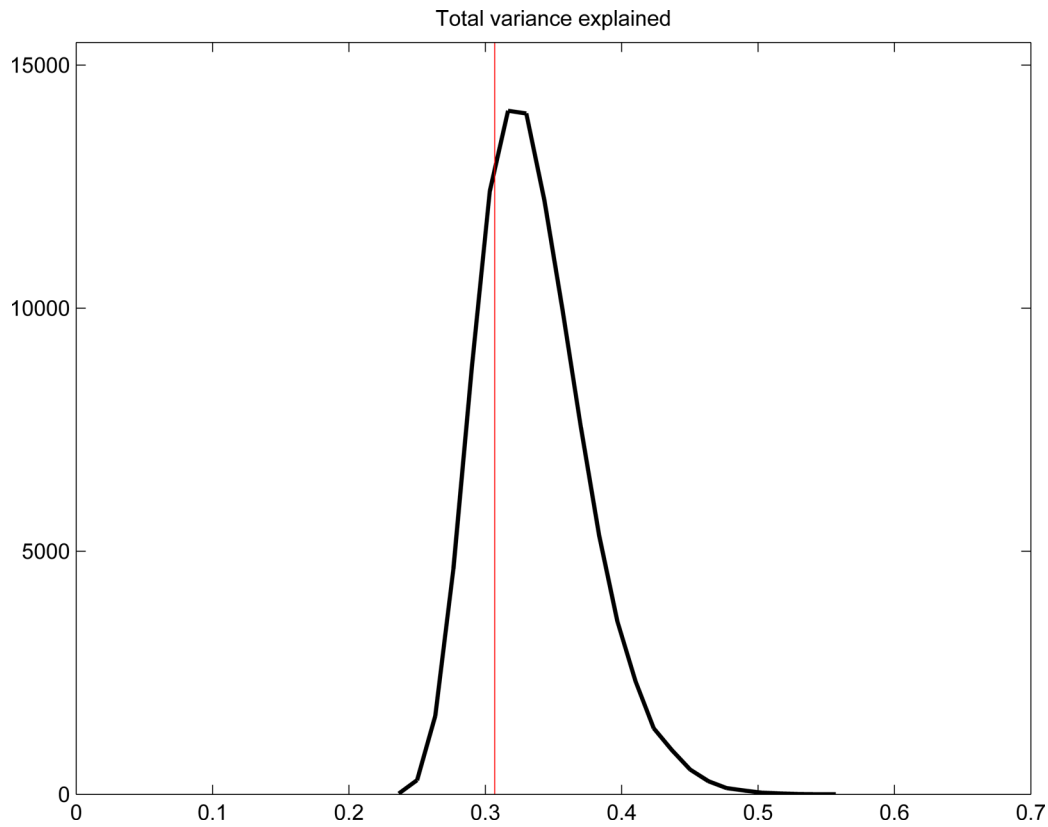
Figure 4. Distribution of the variance explained by the first component of the EOF decomposition of each of 100 000 synthetized sets of seven time-series. The red vertical line is the value of the first EOF obtained with the actual SG data set.

Table 5. Amplitude (in nm s^{-2}) and phases (in days) as shown in Figs 5 and 6, evaluated using least-squares fit of a purely annual term. SG$_{Inv}$ means that the sign at the CO, MB, MO, ST, VI and WA underground stations is inverted. For GRACE, the averages of the different solutions are provided.

Station	SG		SG$_{Inv}$		GLDAS		ERA		GRACE	
	A	Ph	A	Ph	A	Ph	A	Ph	A	Ph
BH	17.2	75.4	17.2	75.4	54.9	61.1	33.5	44.8	18.8	50.8
CO	8.6	112.5	8.6	−67.5	39.7	61.2	18.8	43.4	25.7	69.9
MB	9.8	236.4	9.8	56.4	45.8	46.7	16.6	37.2	16.5	41.5
MC	15.7	34.1	15.7	34.1	57.2	55.1	25.5	41.2	23.0	61.7
MO	0.9	160.3	0.9	−19.7	55.3	57.5	29.7	47.9	19.5	53.8
PE	25.5	64.8	25.5	64.8	42.4	60.5	30.3	56.3	22.9	65.2
ST	7.6	274.5	7.6	94.5	49.7	57.8	29.1	34.5	22.4	56.7
VI	4.6	335.5	4.6	155.5	44.0	56.6	19.8	47.1	25.7	71.2
WA	24.2	290.8	24.2	110.8	59.9	60.6	38.9	40.9	19.3	49.6
WE	29.0	90.4	29.0	90.4	45.1	64.3	25.9	44.7	22.8	62.9

ground water storage, as evidenced by several studies (e.g. Van Camp *et al*. 2006; Meurers *et al*. 2007; Creutzfeldt *et al*. 2008; Longuevergne *et al*. 2009; Lampitelli & Francis 2010; Naujoks *et al*. 2010; Deville *et al*. 2013). Consequently, there is no conclusion to be drawn from either an agreement or a disagreement of amplitude in the seasonal signal. We now focus on the phase, which might be less dependent on the local context and more comparable with large-scale information such as GRACE or climate models.

Fig. 5(b) shows that the phases all are within a time interval of about 222 d; if we restrict our analysis to the largest seasonal signal, between MC and WA, the phases are included in a 77-d interval. This simply means that the maximum water load occurs within a season, which is to be expected. In short, the phase distribution

does not allow concluding that the seasonal signal is common for the available set of SG time-series, but it is consistent with central Europe being wettest at the end of the winter.

4 COMMON VARIABILITY OF SGS, GRACE AND HYDROLOGICAL MODELS

With a resolution of 400 km, GRACE barely distinguishes the position of the different stations and is mostly sensitive to the large-scale feature of the ground water mass distribution. This would advocate for GRACE being consistent with a common signal in the SG time-series, as long as this common signal actually exists, for example, resulting from a large-scale phenomena, and acts similarly on all terrestrial gravity sensors. In the case of the SG time-series, we have
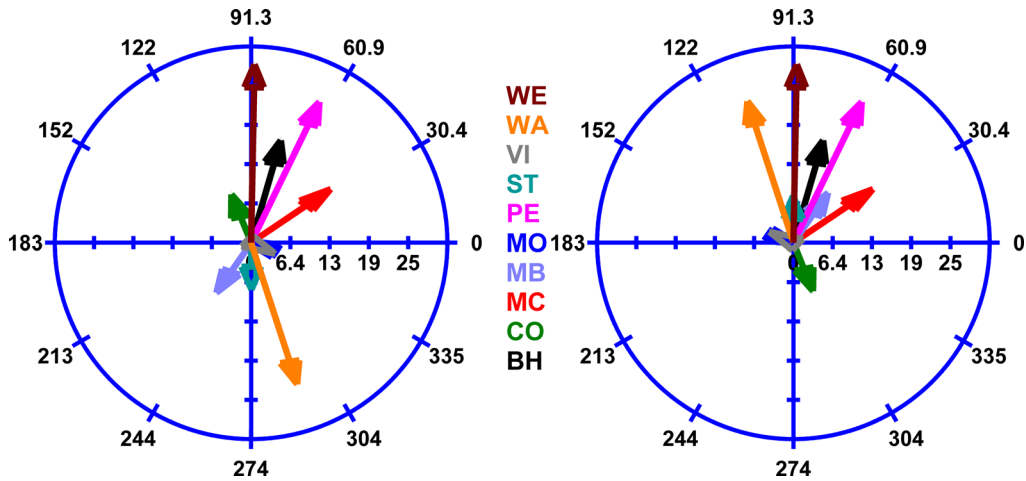
Figure 5. Phasor diagrams of the annual components obtained for the different SG time-series (a) before and (b) after inverting the sign at the CO, MB, MO, ST, VI and WA underground stations. Amplitudes in nm s^{-2}; phases in days.

shown that there is only little, if any, common signal, both at the annual and interannual timescales. This lack of coherence is at least partially caused by diverse site conditions. Nevertheless, as the sub-surface ground water experiences a maximum at the end of the winter, one would expect at least some agreement in phase between the annual component of GRACE, the SG and the hydrological models. This would not imply, considering their transfer functions, that they agree on the water distribution over central Europe; it simply means that they more or less agree that winter is wetter than summer.

Fig. 6 shows the phasor diagrams for the annual component at the different stations for the SGs, the 10 different GRACE solutions and the GLDAS and ERA hydrological models. As, in most cases, hydrology models predict seasonal cycles larger than the other ones, the corresponding arrows are reduced by a factor of 2 for the sake of clarity.

Globally, we see that, as expected, all GRACE solutions are rel-atively close in amplitude and in-phase from within 19 d (CO) to 63 d (MB), but not perfectly identical, depending on the location (at MB, WA and to a lesser extent, ST, there are more differences between the GRACE solutions, probably due to the closeness of the ocean). However, differences between the solutions are glob-ally smaller than the differences between GRACE solutions and hydrology models or SGs.

At all stations but PE and WE, the hydrological models disagree in amplitude, probably partly due to a simplified treatment of near field effects, and only agree within 4 months in phase (Table 5, Figs 6 and 7). For PE and WE, the amplitudes predicted by the ERA model are comparable to the SG observations, although the possible recent changes in the hydrogeological properties around the WE station may have changed this picture.

For three stations located above the ground (BH, MC and PE) and an underground one (MB), there are some phase and/or amplitude agreements between SGs and some of the GRACE solutions, but our sample is too small to draw any real conclusion.

5 LOCAL EFFECTS

Obviously, there are some common signals within the water mass distribution around stations located within a few hundred kilome-tres, and these common signals may be emphasized in the GRACE signal. We have shown that this common signal does not dominate the SG series.
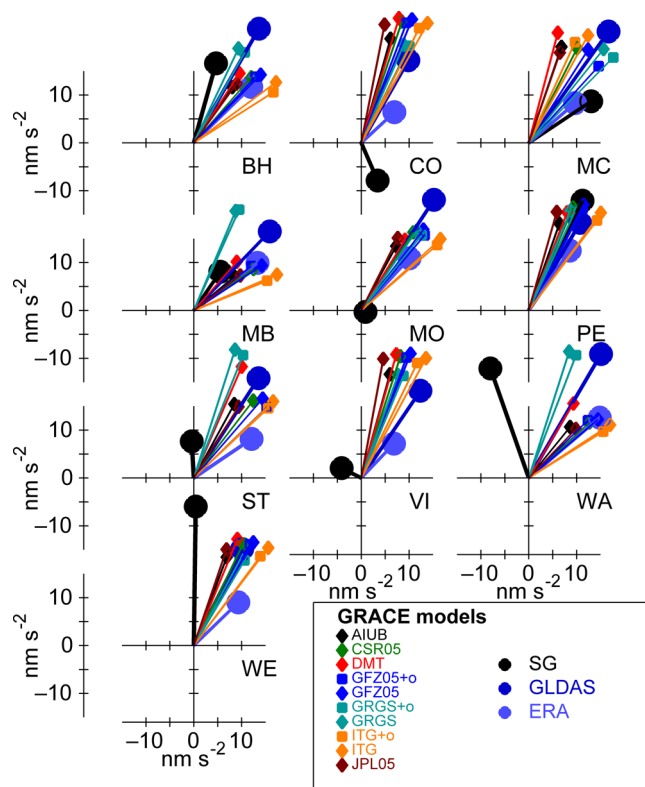

Figure 6. Phasor diagrams of the annual components at the different SG stations for the 10 different GRACE solutions and the two GLDAS and ERA hydrological models. For clarity, the amplitude of the global hydrological models is reduced by a factor 2. The sign of the SG data from the CO, MB, MO, ST, VI and WA underground stations is inverted.

The dominant signal in the SG time-series comes from the area directly around the instrument, within a few hundred metres, as shown, for example, by Creutzfeldt *et al.* (2008). A perfect hydro-logical local model accurately estimates the direct attraction from mass close to the gravimeter but, subtracting it, the corrected gravity signal cannot be consistent with the mass distribution observed by GRACE, as demonstrated in the Appendix. To compare SGs with GRACE, it is necessary to add back $g_{L_{\text{Smooth}}}(S)$, the smoothed local effect of the mass distribution, into the corrected SG series (see eqs A4–A6). One could estimate $g_{L_{\text{Smooth}}}(S)$ by using GRACE or local
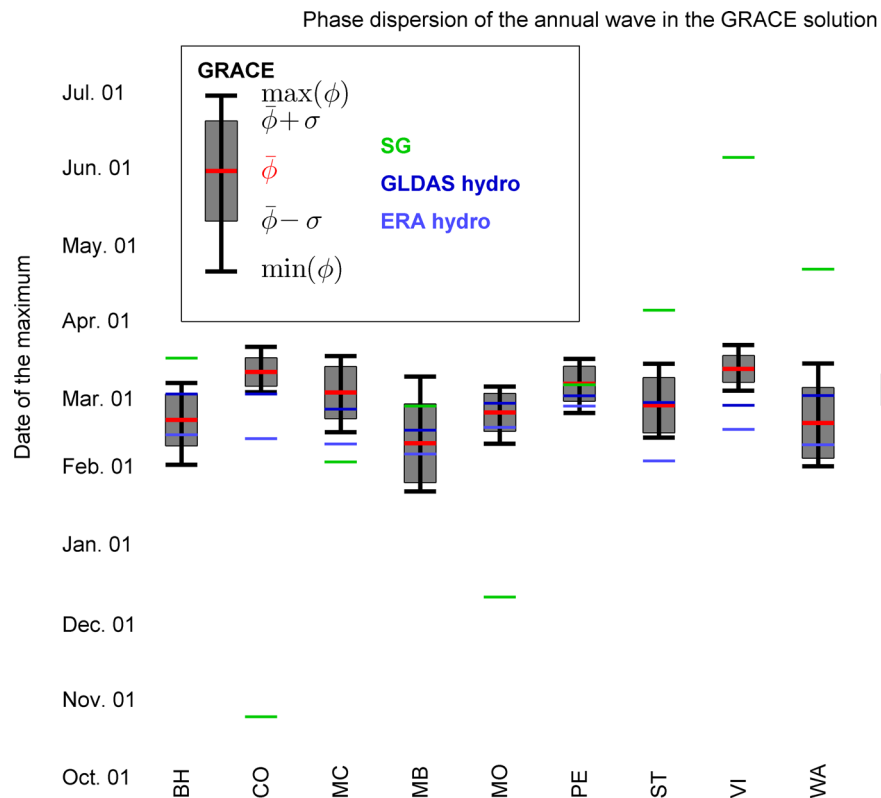
Figure 7. Phase distribution of the annual component in the GRACE solutions, hydrological models and SG time-series at the SG stations. The sign of the SG data from the CO, MB, MO, ST, VI and WA underground stations is inverted. For the GRACE solutions, the whiskers indicate the upper and lower extreme values, as well as the average and the one sigma confidence interval.

models. In the first case, one would create a common signal, even if there is none, which is not appropriate; in the second case, one would have to rely on perfect hydrological models, but then, why using an SG for hydrological investigations?

Our results, and those from previous studies, show that the agreement with GRACE is worse for an underground station; this makes perfect sense considering that the part of the mass closest to the SG is above an underground instrument, which generates a partial cancelation of the signal, as in MO, ST and VI, but not in WA. Obviously, considering those stations as anomalous, as done by Crossley *et al*. 2012, does improve the coherence of the remaining set. Overall, it shows the limitation of the comparison of very local measurements with regional ones.

6 CONCLUSION

At first sight, looking for an agreement between SGs and GRACE is a long shot, as numerous studies have shown that most of the gravity effects recorded by SGs are induced by subsurface water dynamics in a radius around the gravimeter smaller than 1000 m. On the other hand, if successful, there would be much to be learned from the intercomparison in terms of validation, calibration and corrections of geodetic and hydrological measurements.

The analysis of time-series from 10 European SGs showed that (1) except for the presence of an annual cycle at most of the stations, as in most geodetic time-series, there is no clear common behaviour between the different SGs; (2) the consistency between the annual cycles of the different SGs is poor, both in phase and amplitude. Similarly, the annual cycles of the SGs are not consistent with predictions computed from GRACE and hydrological models.

Considering the complexity of the hydrogeological processes governing the conversion between rainfall and water mass distribution, it is easy to justify disagreements both in phase and in amplitude, as observed here. Consequently, our results do not demonstrate that the physical phenomena monitored by the SGs and GRACE are different. On the other hand, a study combining those data sets can only be fruitful if there are at least some degrees of consistency.

Terrestrial gravity measurements can be fruitfully used to perform comprehensive, local hydrogeological investigations, as shown in Wettzell (Creutzfeldt *et al*. 2010) or in the Larzac karstic area (Jacob *et al*. 2010); on the other hand, GRACE has provided numerous information on large-scale hydrological and geodynamic phenomena (Pollitz 2006; Ramillien *et al*. 2008). However, this study shows that the feasibility of joined studies is still unclear, in particular because it is impossible to correct SG data for local phenomena to make them comparable with GRACE observations.

REFERENCES

Abe, M. *et al.*, 2012. A comparison of GRACE-derived temporal gravity variations with observations of six European superconducting gravimeters, *Geophys. J. Int.,* **191**(2), 545–556.

Beutler, G., Jäggi, A., Mervart, L. & Meyer, U., 2010. Gravity field determination at the AIUB—the celestial mechanics approach, *J. Geod.,* **84,** 661–681.

Blewitt, G. & Clarke, P., 2003. Inversion of Earth's changing shape to weigh sea level in static equilibrium with surface mass redistribution, *J. geophys. Res.,* **108**(B6), 2311, doi:10.1029/2002JB002290.

Blewitt, G., Lavallee, D., Clarke, P. & Nurutdinov, D., 2001. A new global mode of Earth deformation: seasonal cycle detected, *Science,* **294,** 2342–2345.

Boy, J.-P. & Hinderer, J., 2006. Study of the seasonal gravity signal in superconducting gravimeter data, *J. Geodyn.,* **41,** 227–233.

Boy, J.-P., Gégout, P. & Hinderer, J., 2002. Reduction of surface gravity data from global atmospheric pressure loading, *Geophys. J. Int.,* **149,** 534–545.

Bruinsma, S.L., Lemoine, J.-M., Biancale, R. & Vales, N. 2009. CNES/GRGS 10-day gravity field models (release 2) and their evaluation, *Adv. Space Res.,* **45**(4), doi:10.1016/j.asr.2009.10.012.

Creutzfeldt, B., Güntner, A., Klügel, T. & Wziontek, H., 2008. Simulating the influence of water storage changes on the superconducting gravimeter of the Geodetic Observatory Wettzell, Germany, *Geophysics,* **73**(6), WA95–WA104.

Creutzfeldt, B., Güntner, A., Wziontek, H. & Merz, B., 2010. Reducing local hydrology from high-precision gravity measurements: a lysimeter-based approach, *Geophys. J. Int.,* **183**(1), 178–187.

Crossley, D., Hinderer, J. & Riccardi, U., 2013. The measurement of surface gravity, *Rep. Prog. Phys.,* **76,** doi:10.1088/0034–4885/76/4/046101.

Crossley, D., de Linage, C., Hinderer, J., Boy, J.P. & Famiglietti, J., 2012. A comparison of the gravity field over Central Europe from superconducting gravimeters, GRACE and global hydrological models, using EOF analysis, *Geophys. J. Int.,* **189**(2), 877–897.

Dahle, C., Flechtner, F., Gruber, C., König, D., König, R., Michalak, G. & Neumayer, K.-H., 2012. GFZ GRACE level-2 processing standards document for level-2 product release 0005, *Scientific Technical Report - Data, Potsdam: Deutsches GeoForschungsZentrum GFZ,* doi:10.2312/GFZ.b103–12020.

Deville, S., Jacob, T., Chéry, J. & Champollion, C., 2013. On the impact of topography and building mask on time varying gravity due to local hydrology, *Geophys. J. Int.,* **192**(1), 82–93.

Dziewonski, A.M. & Anderson, D.L., 1981. Preliminary Referential Earth Model, *Phys. Earth planet. Inter.,* **25,** 297–356.

Farrell, W. E., 1972. Deformation of the Earth by surface loads, *Rev. Geophys. Space Phys.,* **10,** 761–797.

Ghil,, M., Allen, R.M., Dettinger, M.D., Ide, K., Kondrashov, D., Mann, M.E. & Robertson, A., 2002. Advanced spectral methods for climatic time series, *Rev. Geophys.,* **40**(1), doi:10.1029/2001RG000092.

Hartmann, D.L. & Michelsen, M.L., 1989. Intraseasonal periodicities in Indian rainfall, *J. Atmos. Sci.,* **46**(18), 2838–2862.

Hinderer, J., Crossley, D. & Warburton, R.J., 2007. Superconducting gravimetry, in *Treatise on Geophysics,* Vol. 3, pp. 65–122, eds Herring, T. & Schubert, G., Elsevier.

Jacob, T., Bayer, R., Chery, J., Jourde, H. & Moigne, N.L., 2010. Time-lase microgravity surveys reveal water storage heterogeneity of a karst aquifer, *J. geophys. Res.,* **115,** B06402, doi:10.1029/2009JB006616.

Klees, R., Revtova, E.A., Gunter, B.C., Ditmar, P., Oudman, E., Winsemius, H.C. & Savenije,, H.H.G., 2008. The design of an optimal filter for monthly GRACE gravity models, *Geophys. J. Int.,* **175**(2), 417–432.

Kurtenbach, E., Mayer-Gürr, T. & Eicker, A., 2009. Deriving daily snapshots of the Earth's gravity field from GRACE L1B data using Kalman filtering, *Geophys. Res. Lett.,* **36,** L17102, doi:10.1029/2009GL039564.

Lampitelli, C. & Francis, O., 2010. Hydrological effects on gravity and correlations between gravitational variations and level of the Alzette River at the station of Walferdange, Luxembourg. *J. Geodyn.,* **49,** 31–38.

Liu, X., Ditmar, P., Siemes, C., Slobbe, D.C., Revtova, E., Klees, R., Riva, R. & Zhao, Q., 2010. DEOS Mass Transport model (DMT-1) based on GRACE satellite data: methodology and validation, *Geophys. J. Int.,* **181,** 769–788.

Longuevergne, L., Boy, J.-P., Florsch, N., Viville, D., Ferhat, G., Ulrich, P., Luck, B. & Hinderer, J., 2009. Local and global hydrological contributions to gravity variations observed in Strasbourg (France), *J. Geodyn.,* **48,** doi:10.1016/j.jog.2009.09.008.

Meurers, B., Van Camp, M. & Petermans, T., 2007. Correcting gravity time series using rain fall modeling at the Vienna and Membach stations and application to Earth tide analysis, *J. Geod.,* **81**(11), 703–712.

Naujoks, M., Kroner, C., Weise, A., Jahr, T., Krause, P. & Eisner, S., 2010. Evaluating local hydrological modelling by temporal gravity observations and a gravimetric 3D model, *Geophys. J. Int.,* **182**(1), 233–249.

Neumeyer, J. *et al.*, 2006. Combination of temporal gravity variations resulting from superconducting gravimeter (SG) recordings, GRACE satellite observations and hydrology models, *J. Geodyn.,* **79,** 573–585.

Neumeyer, J., Barthelmes, F., Kroner, C., Petrovic, S., Schmidt, R., Virtanen, H. & Wilmes, H., 2008. Analysis of gravity field variations derived from superconducting gravimeter recordings, GRACE satellite and hydrological models at selected European sites, *Earth Planets Space,* **60**(5), 505–518.

Pollitz, F., 2006. A new class of earthquake observations, *Science,* **313**(5787), 619–620.

Preisendorfer, R.W., 1988. *Principal Component Analyses in Meteorology and Oceanography,* Elsevier.

Ramillien, G., Famiglietti, J.S. & Wahr, J., 2008. Detection of continental hydrology and glaciology signals from GRACE: a review, *Surv. Geophys.,* **29**(4), 361–374.

Rodell, M. *et al.*, 2004. The global land data assimilation system, *Bull. Am. Meteorol. Soc.,* **85,** 381–394.

Slichter, L.B., 1961. The fundamental free mode of the Earth's inner core, *Science,* **47,** 186–190.

Swenson, S.C. & Wahr, J., 2006. Post-processing removal of correlated errors in GRACE data, *Geophys. Res. Lett.,* **33,** L08402, doi:10.1029/2005GL025285.

Tesmer, V., Steigenberger, P., van Dam, T. & Gürr, T.M., 2011. Vertical deformations from homogeneously processed GRACE and global GPS long-term series, *J. Geod.,* **85**(5), 291–310.

Tregoning, P. & Watson, C., 2009. Atmospheric effects and spurious signals in GPS analyses, *J. geophys. Res.,* **114,** B09403, doi:10.1029/2009JB006344.

Uppala,, S.M. *et al.*, 2005. The ERA-40 re-analysis, *Q. J. R. Meteorol. Soc.,* **131,** 2961–3012.

Valty, P., de Viron, O., Panet, I., Van Camp, M. & Legrand, J., 2013. Assessing the precision in loading estimates by geodetic techniques in Southern Europe, *Geophys. J. Int.,* **194**(3), 1441–1454.

Van Camp, M. & Francis, O., 2006. Is the instrumental drift of superconducting gravimeters a linear or exponential function of time? *J. Geod.,* **81**(5), 337–344.

Van Camp, M., Métivier, L., de Viron, O., Meurers, B. & Williams, S.D.P., 2010. Characterizing long-time scale hydrological effects on gravity for improved distinction of tectonic signals, *J. geophys. Res.,* **115**(B7), B07407, doi:10.1029/2009JB006615.

Van Camp, M., Vanclooster, M., Crommen, O., Petermans, T., Verbeeck, K., Meurers, B., van Dam, T. & Dassargues, A., 2006. Hydrogeological investigations at the Membach station, Belgium, and application to correct long periodic gravity variations, *J. geophys. Res.,* **111,** B10403, doi:10.1029/2006JB004405.

van Dam, T., Wahr, J. & Lavallée, D., 2007. A comparison of annual vertical crustal displacements from GPS and Gravity Recovery and

Climate Experiment (GRACE) over Europe, *J. geophys. Res.,* **112,** B03404, doi:10.1029/2006JB004335.

Von Storch, H. & Zwiers, F.W., 1999. *Statistical Analysis in Climate Research,* Cambridge Univ. Press, 484 pp.

Wahr, J., 1985. Deformation induced by polar motion, *J. geophys. Res.,* **90**(B11), 9363–9368.

Weise, A., Kroner, C., Abe, M., Ihde, J., Jentzsch, G., Naujoks, M., Wilmes, H. & Wziontek, H., 2009. Gravity field variations from superconducting gravimeters for GRACE validation, *J. Geodyn.,* **48,** 325–330.

Weise, A. *et al.*, 2011. Tackling mass redistribution phenomena by time-dependent GRACE- and terrestrial gravity observations, *J. Geodyn.,* **59**(SI), 82–91.

Wenzel, H.-G., 1996. The nanogal software: Earth tide data processing package ETERNA 3.30., *Bull. Inf. Marées Terrestres,* **124,** 9425–9439.

APPENDIX: COMPARISON OF THE TERRESTRIAL AND SATELLITE OBSERVATIONS OF HYDROLOGICAL EFFECTS ON GRAVITY

Let us consider three hydrologic units, as shown in Fig. A1:

1. R remote (light blue);
2. L local (dark blue);
3. L_{Smooth} local, where the water mass contained in the L unit is smoothed by the GRACE transfer function (hatched).

The water contained in L participates to the mass distribution that is observed by GRACE.

Then, we have:

1. g_D: gravity signal caused by the ground displacement due to the loading effect;
2. g_R: gravity signal caused by the Newtonian effect from the remote mass in the R unit;
3. g_L: gravity signal caused by the Newtonian effect from the local mass in the L unit.

These quantities are understood as projection of their corresponding vectors onto the vertical direction.

The gravity measured by the SG at the surface station S reads as

$$g_{\text{SG}}(S) = g_D + g_R(S) + g_L(S). \tag{A1}$$

The gravity measured by the SG at the underground station U reads as

$$g_{\text{SG}}(U) = g_D + g_R(U) + g_L(U). \tag{A2}$$

If the distance r to the limit of the global domain R is large compared to the distance between points S and U, we have

$$h(S) - h(U) \ll r,$$

and

$$g_R(U) \cong g_R(S).$$

Such that (A2) becomes

$$g_{\text{SG}}(U) \cong g_D + g_R(S) + g_L(U). \tag{A3}$$

The gravity as measured by GRACE, reconstructed at the SG station location S as a ground gravity value, reads as

$$g_{\text{GRACE}}(S) = g_D + g_R(S) + g_{L_{\text{Smooth}}}(S). \tag{A4}$$

To make a meaningful comparison between GRACE and SG, we have included the deformation part g_D deduced from the GRACE load models in the estimation of $g_{\text{GRACE}}(S)$.

$g_{L_{\text{Smooth}}}(S)$ is the gravity effect from the water contained in the L unit, reconstructed at the S site. The equivalent water height is of the same order of magnitude as in the R unit, although the gravity effect $g_R(S)$ turns out to be small as that water is far from S.

If the topography of L is flat and the water contained in L is homogeneously distributed within L, the water mass in L and the water mass in L_{Smooth} would be similar and $g_L \cong g_{L_{\text{Smooth}}}$. On the other hand, if the same total water mass is concentrated in a small region within L, then the mass in L would be far larger than in L_{Smooth} and $g_L \gg g_{L_{\text{Smooth}}}$. Hence, the GRACE signal would be dominated by $g_D + g_R$, and the SG signal by g_L. Yet, in this case, even if GRACE and SG see different sources, the signal maxima would be within 3 months because all water sources present seasonal variations.

Taking (A3) and (A4) into account, the correction for making SG gravity comparable with GRACE requires applying a remove–restore technique (bold):

$$g_{\text{SG,compar}}(S) = g_{\text{SG}}(S) - \boldsymbol{g_L(S)} + \boldsymbol{g_{L_{Smooth}}(S)}, \tag{A5}$$

$$g_{\text{SG,compar}}(U) = g_{\text{SG}}(U) - \boldsymbol{g_L(U)} + \boldsymbol{g_{L_{Smooth}}(S)}. \tag{A6}$$

These equations show that it is only possible to convert g_{SG} to something that we can compare with GRACE if we know, by some other means, the mass everywhere around the gravimeter.
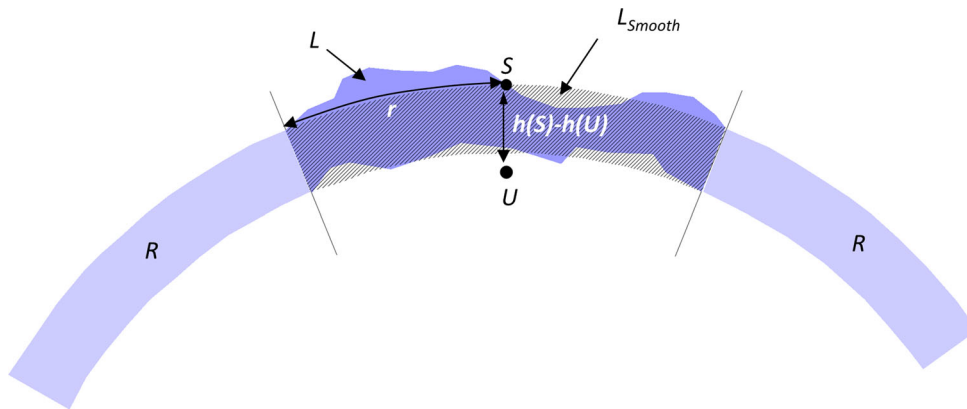

Figure A1. The three different hydrologic units R, L and L_{Smooth} taken into account when investigating hydrological effects on satellite and terrestrial gravity measurements. Note that the location of U shown here is exemplary. U can be located below the surface anywhere, within or below the L unit.